Electronic Supplementary Information for the article

Exploiting level anti-crossings for efficient and selective transfer of hyperpolarization in coupled nuclear spin systems

Andrey N. Pravdivtsev,[a,b] **Alexandra V. Yurkovskaya,**[a,b] **Robert Kaptein,**[b,c] **Karsten Miesel,**[d] **Hans-Martin Vieth**[d] **and Konstantin L. Ivanov***[a,b]

[a] *International Tomography Center SB RAS, Novosibirsk, 630090, Russia. Fax: +7(383)333-1399; Tel: +7(383)333-3861; E-mail:ivanov@tomo.nsc.ru;*
[b] *Novosibirsk State University, Novosibirsk, 630090, Russia;*
[c] *Utrecht University, NL-3584 CH, Utrecht, the Netherlands;*
[d] *Freie Universität Berlin, Berlin, 14195, Germany.*

The ESI includes:
Low-field CIDNP transfer data for Subsystem 1
Low-field CIDNP transfer data for Subsystem 2
Field dependence of proton T_1-relaxation times

Low-field CIDNP transfer

Polarization transfer in Subsystem 1

In the main text we discussed polarization transfer for Subsystem 1 of N-Ac-Trp at the LAC field of 0.313 mT. Here we describe the situation at zero field where selective CIDNP transfer occurs between the $\beta1$-CH_2 proton and the H2 proton. It is readily seen (Figure 1S) that the oscillations have the same frequency but opposite phase for the two protons. This is a clear indication that they are involved together in the polarization exchange. When relaxation effects are taken into account, the simulation is in very good agreement with the experimental curves. The frequency of the oscillations is approximately 1 Hz. Although only a single frequency is predominant in the time traces shown in Figure 1S the situation is rather complex. This is because for the four-spin system under consideration there are more than two levels exchanging population; consequently, more than one coherence is excited. Our theoretical analysis shows that the initial difference of state populations at high field allows one to excite several coherences by field variation. However, splittings between the corresponding levels are very similar at zero field: the time evolution therefore exhibits a single apparent frequency of oscillation. The analysis also shows that although all four protons are involved in the CIDNP transfer, polarization exchange is the most pronounced for the $\beta1$-CH_2 and the H2 protons, which is consistent with the observation.
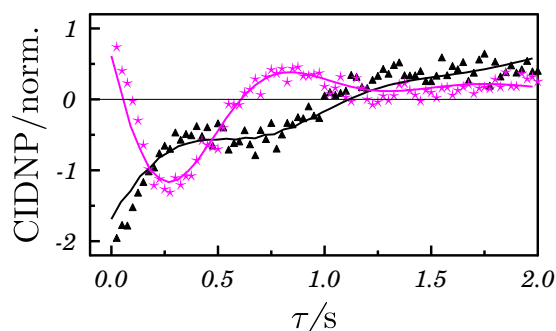

Figure 1S. Time-dependent CIDNP transfer in N-Ac-Trp between the H2 proton (asterisks, magenta) and $\beta1$-CH_2 proton (filled triangles, black) at $B_{int} = 0$. Theoretical calculations are shown by solid lines.

Polarization transfer in Subsystem 2

CIDNP after two field jumps as a function of τ, is shown in Figure 2S for three magnetic fields B_{int}. In all cases coherent polarization exchange is seen, in which all four protons are involved, not just two as one may expect from the field dependence shown in Figure 6a (polarization exchange between H5-H6 is much weaker). The oscillations in the time traces have opposite phases for the pairs H4-H7 and H5-H6; in the time dependence there are only a few frequencies present. Excellent agreement between the calculation and experiment facilitates the theoretical analysis and opens a way to map out coherences that are responsible for the observed transfer effects. Since the amplitudes and frequencies of coherences, which are excited by the $B_0 \rightarrow B_{int}$ field jump, are correctly reproduced, we assign the observed frequencies to coherences between particular pairs of spin states. This was done in the following way: we first calculated the amplitudes of all coherences at $B = B_{int}$ right after the first field variation (*i.e.*, at $\tau = 0$). Next, the ZQCs with high amplitudes were selected, and then the corresponding pairs of eigen-states at low field B_{int} were assigned to the high-field eigen-states. Exactly these pairs of

states (indicated in Figure 6b) can exchange populations due to the presence of LACs.
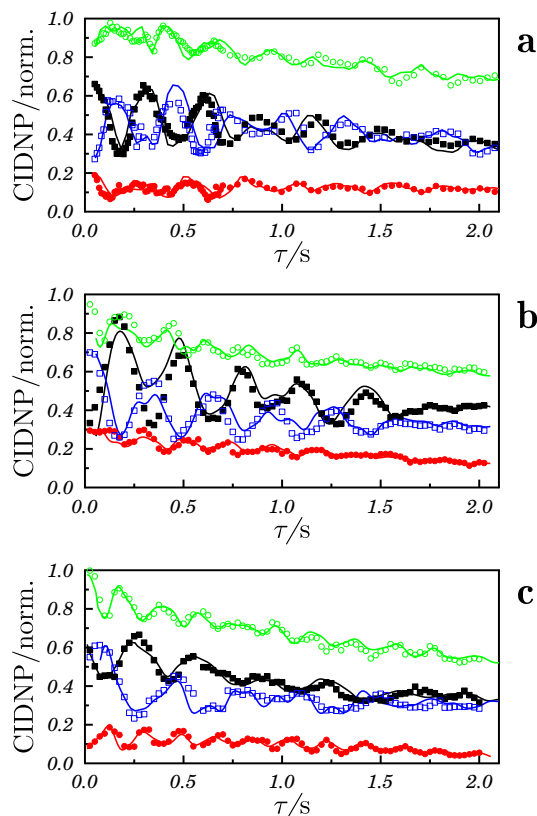

Figure 2S. Time-dependent CIDNP transfer between the H4, H5, H6 and H7 protons at different B_{int}: 47 mT (a); 180 mT (b); 313 mT (c). Solid lines show results of theoretical calculation; polarization is denoted by black filled squares (H4 proton), red filled circles (H5 proton), green open circles (H6 proton), and blue open squares (H7 proton).

In fact, in this system we never met conditions for selective CIDNP transfer for other pairs of protons, for instance, for the H4-H5 pair. This is because the coherent pathways, which can transfer polarization in the other pairs of spins, are not operative, since our maximum speed of field switching is too low to be non-adiabatic for the corresponding LACs. In general, when the field variation can be performed faster (for instance, two times faster than we can do it now), it is possible to excite all ZQCs. Then, by properly setting the delay at $B = B_{int}$ it is possible to manipulate the phase of the coherences and in this way optimize the polarization transfer within a selected pair of spins.

To investigate the rate of field-cycling in polarization transfer experiments further we also performed experiments with slow (adiabatic) field variation. In this case (not shown here) no exchange of polarization was observed; there was only a decay of polarization caused by spin relaxation. This is in agreement with the qualitative consideration of adiabatic field cycling: the spin eigen-states keep their populations all the time, so that they remain the same after two field variations. No spin coherences are created in this case. This shows that the transfer mechanism is operative only when the field variation is non-adiabatic.

The CIDNP transfer between the H4 and H7 protons is most efficient at magnetic fields of about 150 mT although there is a LAC not only at this field but also at zero, 270 mT, 370 mT and 1.2 T. To explain this observation we performed additional experiments. First, we studied the time-dependent CIDNP transfer at several magnetic fields B_{int} (see Fig. 7 and 2S) in order to reveal coherent effects, analyze the transfer frequencies and identify particular coherences, which

are responsible for the polarization transfer. Second, we investigated the field dependence of the CIDNP transfer efficiency at different timing for stages 2-4. As a result, we found that the peak in the transfer efficiency may not coincide with the LAC position, B_{lac}. This is because when B_{int} is lower than B_{lac} (the condition $B_{lac} > B_{int} > 0$ can always be fulfilled for systems of three or more spins), the spin system passes through the LAC twice in the course of the experimental protocol. In this situation ZQCs are excited efficiently and they evolve during the field variations $B_{lac} \rightarrow B_{int}$ and $B_{int} \rightarrow B_{lac}$. The experimental timing considerably affects the resulting polarization transfer pattern. Moreover, due to the fact that the evolution is coherent the dependence on the times of the field cycling $B_{lac} \rightarrow B_{int}$ and $B_{int} \rightarrow B_{lac}$ is not monotonous. As a consequence, the maximum of the polarization transfer efficiency can be shifted from B_{lac} to a lower field. The position of this 'optimal' field depends on the timing of the experiment, namely, on the time periods τ_1, τ and τ_2 and, moreover, on the field variation profile of both field switches.

T_1-relaxation of protons in N-Ac-Trp

T_1-relaxation time of the CH_3 protons is field-independent (Figure 3S) because they are completely decoupled from the rest of the molecule. In contrast to this trivial case, in the coupled proton subsystems we see pronounced features in the relaxation dispersion. In both subsystems spins relax with a common T_1 at low fields. In the system composed of the α-CH, β-CH_2 and H2 protons (Figure 3Sa) there are sharp features caused by LACs at ≈0.3 T (LAC in the three-spin system formed by the α-CH and β-CH_2 protons) and at ≈60 and 80 mT resulting from coupling of all the four spins. In the other four-spin system the features coming from LACs are much less pronounced (Figure 3Sb) because for these spins the longitudinal relaxation times in the limit of weak coupling (intrinsic T_1-relaxation times) have a much smaller difference. Experimental observations are in very good agreement with theoretical calculations, which were done in the way described previously with two additional simplifications: (i) we considered only relaxation of state populations and (ii) neglected effects of field variation on the T_1-relaxation times observed at high field. As is clearly seen these two assumptions are not crucial with the result that the calculation very well reproduces the experimental observation (Figure 3S).
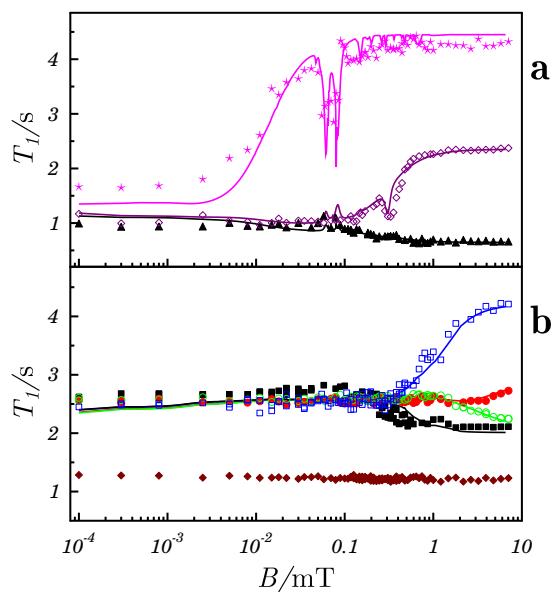

Figure 3S. Field dependence of T_1-relaxation times (relaxation dispersion) of Trp protons: α-CH proton (open diamonds, purple), β-CH_2 protons (filled triangles, black) and H2 proton (asterisks, magenta) – subplot (a); H4 proton (filled squares, black), H5 proton (filled circles, red), H6 proton (open circles, green), H7 proton (open squares, blue) and CH_3 protons (filled diamonds, brown) – subplot (b). Solid lines show results of theoretical calculation.

3

Table 1S. Constants of spin-spin coupling, J_{ij}, and chemical shifts, δ_i, of N-acetyl-tryptophan at pH=5.2. T_1 relaxation times of protons, T_{1i}, and their starting polarizations, M_i, measured at 7 T are also presented.

J_{ij}, Hz	$\beta 1$-CH_2	$\beta 2$-CH_2	α-CH	H2	H4	H5	H6	H7
$\beta 1$-CH_2		–	–	–	–	–	–	–
$\beta 2$-CH_2	–14.8		–	–	–	–	–	–
α-CH	4.9	7.8		–	–	–	–	–
H2	–0.7	–0.8			–	–	–	–
H4	–	–	–	–		–	–	–
H5	–	–	–	–	8		–	–
H6	–	–	–	–0.4	1.2	7		–
H7	–	–	–	–	–0.8	1.1	8.3	
δ_i, ppm	3.3110	3.0960	4.495	7.168	7.6360	7.1150	7.1850	7.4340
T_{1i}, s	0.7	0.7	4	6.2	2.7	2.7	2.4	5.8
M_i, a.u.	–0.23	–0.18	0	0.4	1	–0.1	0.74	0.08